

Clothes-Invariant Feature Learning by Causal Intervention for Clothes-Changing Person Re-identification

Xulin Li^{1*}, Yan Lu^{2*}, Bin Liu^{1†}, Yuenan Hou², Yating Liu¹, Qi Chu¹, Wanli Ouyang², Nenghai Yu¹
¹University of Science and Technology of China, ²Shanghai AI Laboratory

Abstract

Clothes-invariant feature extraction is critical to the clothes-changing person re-identification (CC-ReID). It can provide discriminative identity features and eliminate the negative effects caused by the confounder—clothing changes. But we argue that there exists a strong spurious correlation between clothes and human identity, that restricts the common likelihood-based ReID method $P(Y|X)$ to extract clothes-irrelevant features. In this paper, we propose a new Causal Clothes-Invariant Learning (CCIL) method to achieve clothes-invariant feature learning by modeling causal intervention $P(Y|do(X))$. This new causality-based model is inherently invariant to the confounder in the causal view, which can achieve the clothes-invariant features and avoid the barrier faced by the likelihood-based methods. Extensive experiments on three CC-ReID benchmarks, including PRCC, LTCC and VC-Clothes, demonstrate the effectiveness of our approach, which achieves a new state of the art.

1. Introduction

Person re-identification (ReID) [6, 20, 28, 41] aims to retrieve specific pedestrians across different scenarios, which is widely used in city security surveillance. It is challenging due to the existence of frequent occlusion, background interference and camera view changes. Significant progress has been observed on standard person ReID assuming persons do not change their clothes in the whole retrieval process, which, however, leaves great challenges for the clothes-changing ReID (CC-ReID).

In CC-ReID, clothes-invariant feature learning is of great importance, where the learned discriminative features should be robust to clothes changes. However, it is non-trivial to learn clothes-invariant features since there exists a **strong clothes-identity spurious correlation**. The correlation between clothes and human identity is caused by several potential biases, *e.g.*, the diversity of clothing types. Because of the large number of clothes types all over the world, there is a small probability for us to meet one person wearing the same clothes as us. Moreover, gender, body

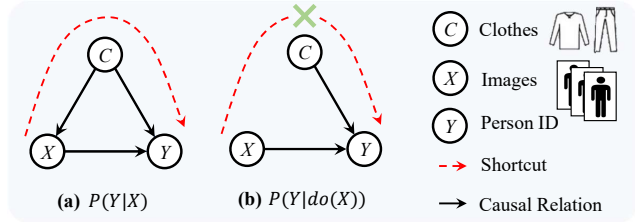


Figure 1. (a) The structural causal model for clothes C , images X and person identity (ID) Y for CC-ReID. The red dash arrow shows the shortcut $X \dashrightarrow C \dashrightarrow Y$ captured by the likelihood-based methods that directly utilize $P(Y|X)$ to model the relationships from X to Y . (b) Our method models the relationships from X to Y by the causal intervention probability $P(Y|do(X))$, which only captures the causal relation $X \rightarrow Y$ and removes the shortcut. Here, $do(\cdot)$ denotes the causal intervention operation [5, 22].

type, and personal preferences further enhance such strong individuality of clothing styles. This property is naturally reflected in the CC-ReID datasets – the same outfits are only worn by one person and never shared with others. Besides, since each person only wears a small number of clothes, this spurious correlation will be further strengthened.

To illustrate the influence of such clothes-identity spurious correlation more clearly, we formulate the causalities among ‘images’ X , ‘human ID’ Y , and confounder ‘clothes’ C as a Structural Causal Model (SCM) [5, 22], as shown in Figure 1 (a). The solid direct links in Figure 1 denote the causal relationships: cause \rightarrow effect. $X \rightarrow Y$ means that the human ID is estimated from the given image and $C \rightarrow X$ indicates that different clothes lead to different image contents. $C \rightarrow Y$ means the identity can be inferred from the clothes, which corresponds to the aforementioned spurious correlation. In summary, there are two relationships from X to Y : a **shortcut** $X \dashrightarrow C \dashrightarrow Y$ and a **causal relation** $X \rightarrow Y$. Note that \dashrightarrow just means the variable computational order in the model learning patterns but does not reflect the causality. Obviously, the objective of clothes-invariant feature learning is to eliminate the shortcut and capture the causal relationship. However, the shortcut and the causal relationship are entangled together. For a likelihood-based model $P(Y|X)$ which directly models the relationship between the X and Y , the shortcut will be captured unavoidably. Besides, because of the abstract modeling property of deep neural networks, the learned patterns of

*Equal contribution.

†Corresponding author.

the shortcuts are represented in an implicit and unexplainable way. Therefore, once the clothes shortcut is captured by the model, it is quite difficult to remove its corresponding patterns from the model and not affect the useful knowledge related to the causal relationships simultaneously.

To handle the difficulties above, we propose to achieve the clothes-invariant feature learning in a causal inference manner. As opposed to the likelihood-based model $P(Y|X)$, the causality-based model aims to model the intervention probability $P(Y|do(X))$, where $do(\cdot)$ denotes the intervention operation [5, 22]. The main advantage of the intervention can be seen from the following equation:

$$P(Y|do(X)) = \sum_j P(Y|X, C = c_j) \cdot P(C = c_j), \quad (1)$$

where summarizing j means traversing all clothes in the training data. This equation is the modern definition of the intervention probability, called backdoor adjustment [5, 22]. Comparing with the original likelihood probability:

$$P(Y|X) = \sum_j P(Y|X, C = c_j) \cdot P(C = c_j|X). \quad (2)$$

It can be found that the backdoor adjustment modified the $P(C = c_j|X)$ to $P(C = c_j)$, which is equal to making clothes C statistically independent of images X . So, $C \rightarrow X$ in Figure 1 (a) is eliminated and the whole figure transfers to Figure 1 (b). Under that, the shortcut $X \dashrightarrow C \dashrightarrow Y$, identifying persons by recognizing corresponding clothes, is not available because X and C become independent. With this design, we only retain the causal relation $X \rightarrow Y$ and realize the clothes-invariant features. To this end, we propose a novel Causal Clothes-Invariant Learning (CCIL) to achieve such intervention in the feature learning process. The main design of our CCIL is mainly concentrated on how to implement the intervention.

CCIL consists of a Clothes-Identity Disentangle Network (CIDNet) and a Clothes-Changing Causal Intervention module (C^3I). The CIDNet plays the role of feature extractor to represent the clothes C and image X in the causal model, respectively. It extracts discriminative and disentangled clothes features and image features through the effective design of network structure and loss function. After the feature extraction, the C^3I module is proposed to compute the $P(Y|do(X))$ by the 'backdoor adjustment' based on those features following the Equation 1. The whole feature learning process is formulated under the causal intervention framework, leading to clothes-invariant feature extraction.

Our main contributions are summarized as follows:

- We analyze the barrier of clothes-invariant feature learning in CC-ReID and propose a novel method dubbed Causal Clothes-Invariant Learning (CCIL) to treat it from the causal inference view.
- To implement the CCIL, we propose the Clothes-Identity Disentangle Network (CIDNet) and the Clothes-Changing Causal Intervention Module (C^3I) to model the $P(Y|do(X))$ effectively.
- Extensive experiments on three public benchmarks show that our CCIL achieves a new state of the art for CC-ReID, which demonstrates the effectiveness of our method.

2. Related Work

Cloth-Changing Person ReID. Standard person re-identification (ReID) [6, 20, 27, 28, 41] aims to retrieve persons of interest across non-overlapping cameras. Many methods have been proposed to address viewpoint variations [14], low-image resolutions [34], illumination changes [12], poses variations [26] and occlusions [10]. However, these methods are limited by the situation where people change their clothes. So, the Clothes-changing person re-identification (CC-ReID) task has attracted increasing attention in recent years. Most existing CC-ReID methods use extra clothes-invariant modality data to guide model training. Yang *et al.* [36] used pure contour sketches for discriminative feature learning. Chen *et al.* [3] directly extracted a texture-insensitive 3D shape embedding from a 2D image by adding 3D body reconstruction as an auxiliary task. Hong *et al.* [9] used 2D silhouettes, Qian *et al.* [24] introduced keypoints, and Jin *et al.* [13] utilized gait to assist better clothes-invariant features learning.

Other methods [7, 11, 32, 38] only use the original RGB image to solve CC-ReID. Huang *et al.* [11] proposed a clothing status awareness method, to enhance the robustness of retrieving unknown dressing states person. Wan *et al.* [32] extracted local face features and fuses them with holistic features to increase the weight of clothing-invariant cues. Yu *et al.* [38] proposed a new clothing templates-based retrieval setting and implemented it by a two-branch Biometric-Clothes network. Gu *et al.* [7] proposed a simple adversarial loss to decouple clothes-irrelevant features from the RGB modality, achieving advanced performance by introducing a well-designed feature learning constraint. However, these methods are most essentially likelihood-based methods, inevitably suffering from the clothes-identity spurious correlation, making their representation carry clothes-related patterns. In contrast, our approach aims to solve clothes-invariant feature learning by the causality view, which is inherently invariant to the confounder—clothes, bringing more discriminative clothes-invariant features.

Causal Inference. Recently, improving deep learning through causal inference has received increasing attention. Thanks to its powerful ability to remove bias and pursue causal effects [1], it has been applied to various fields in computer vision, including image classification [2, 19, 29], visual dialog [23], visual question answering [21], semantic segmentation [39], object detection [33, 40] and scene graph generation [30]. Some work attempted to combine causal inference with person re-identification. Rao *et al.* [25] presented a counterfactual attention learning method to improve visual attention learning. Li *et al.* [17] calculated the total indirect effect to highlight the role of graph topology in the whole training process, achieving new state of the arts on their tackling ReID topics. There is still no causal method for CC-ReID. In this paper, we propose a novel causality-based clothes-invariant learning method for CC-ReID and achieve a new state of the art.

3. Causal Clothes-Invariant Learning

Overview. The main pipeline of our Causal Clothes-Invariant Learning (CCIL) is shown in Figure 2. The input image is first sent to the Clothes-Identity Disentangle Network (CIDNet) to extract clothing and image features (Section 3.1). At the inference stage, we use the image features from the CIDNet as the human signature and directly measure cosine similarities across humans to obtain the retrieval results. At the training stage, clothing and image features are then fed into the proposed Causal Cloth-Changing Intervention (C^3I) module (Section 3.3) to compute the intervention probability $P(Y|do(X))$. The C^3I module guides the model to capture the causal relationship between image and human identity while neglecting the shortcut of identifying humans by recognizing their clothes, leading to purer clothes-invariant features.

3.1. Clothes-Identity Disentangle Network

We design a Clothes-Identity Disentangle Network (CIDNet) to extract the human and clothes features simultaneously. As shown in Figure 2, for a given image, we extract the image feature f_{img} and a corresponding clothes feature f_{clt} by a two-stream network.

Feature extraction. The RGB image is first fed into a fully-convolutional module to produce feature maps. The feature maps are then sent to two specific branches to generate the clothes and image feature maps, written as $m_{clt} \in \mathbb{R}^{H \times W \times C}$ and $m_{img} \in \mathbb{R}^{H \times W \times C}$, respectively, where $H \times W \times C$ is the size of the feature maps.

S^2M Module. To make clothes and image features cover different kinds of information, we propose a Spatial Separate Module (S^2M) to guide two kinds of feature maps focus on different spatial regions by an attention mechanism:

$$\begin{aligned} m'_{img} &= A_{img} \odot (1 - A_{clt}) \odot m_{img}, \\ m'_{clt} &= A_{clt} \odot (1 - A_{img}) \odot m_{clt}, \end{aligned} \quad (3)$$

where $A_{img} \in \mathbb{R}^{H \times W}$ and $A_{clt} \in \mathbb{R}^{H \times W}$ denote the spatial attention maps of the image and clothing features, which are generated by adding 1×1 convolution to the m_{img} and m_{clt} respectively, indicating the important region that each kind of feature map aims to attend. m' is the updated feature maps and the process of Equation 3 means that each kind of feature map is multiplied by its own attention map and the reverse map of the other, which means only preserving the intersection region of the current branch focusing and the other branch neglecting. That keeps regions attended by different kinds of feature maps mainly different. We construct the S^2M module twice on the feature maps to further accomplish the aforementioned goal, making different kinds of feature maps cover different semantic information. After obtaining the two kinds of feature maps, the average pooling module is utilized to process two kinds of feature maps to aggregate the spatial information. The average-pooled outputs are the final image and clothes feature vectors, f_{img} and f_{clt} respectively. The f_{img} is used during inference to retrieve targets for ReID.

Discussion about disentangling target. The target of CIDNet is to separate the clothes and image information from the given image. A standard understanding of such disentanglement is to extract pure clothes and image features so that the image features can reflect the human identity better. However, under the causal intervention learning framework, disentanglement plays other roles, fulfilling the potential requirements of the causal intervention implementation. Details can be shown in § 3.3.2.

3.2. Overall Optimization

3.2.1 Disentanglement feature learning

For the input image x_i , we extract two kinds of features. To make image feature f_{img} identity-discriminative and clothes feature f_{clt} clothes-discriminative, we utilize the cross-entropy loss to train the model under classification tasks that image features predict the human identity and the clothes features estimate the clothes type:

$$\mathcal{L}_{cls} = \mathcal{L}_{ce}(p_{img}) + \mathcal{L}_{ce}(p_{clt}), \quad (4)$$

where p_{img} and p_{clt} denote the predicted classification results computed by corresponding image and clothes features. This classification loss ensures the basic discriminativeness of these two kinds of features.

To keep the disentangled property of such two kinds of features, we propose a Joint Prediction Scheme (JPS) that mixes the clothes and image space together. Specifically, assuming we have N human and M clothes types, we do not directly let the image feature predict the N identity distributions and the clothes feature computes M clothes category distributions. We make both kinds of features predict the $N + M$ category distributions so that clothes and images are turned into negative categories of each other. In this condition, the ground truth one-hot vector to train the classification is also turned into a $N + M$ one. For the image features, the positive index must be located at the first N elements, and the clothes positive index is must set in the last N elements. This strategy further enhances that the clothes features should have different information from the image ones, leading to better disentanglement.

Besides, to further increase the discriminativeness of features, we employ an additional KL-divergence loss function \mathcal{L}_{kl} and a metric learning loss \mathcal{L}_{me} . \mathcal{L}_{kl} aims to reduce the intra-class variance of classification:

$$\mathcal{L}_{kl} = \mathbb{E}[D_{KL}(p_{img}||p'_{img}) + D_{KL}(p_{clt}||p'_{clt})], \quad (5)$$

where $D_{KL}(\bullet||\bullet)$ implies the KL divergence. p'_{img} is the classification center computed by averaging the classification confidence across samples that have the same class as the current input image. And p'_{clt} has a similar meaning. So this term means that the classification confidence between different positive samples should be as similar as possible. And \mathcal{L}_{me} is a contrastive-liked metric learning loss that guides the features close to the positive centers and far

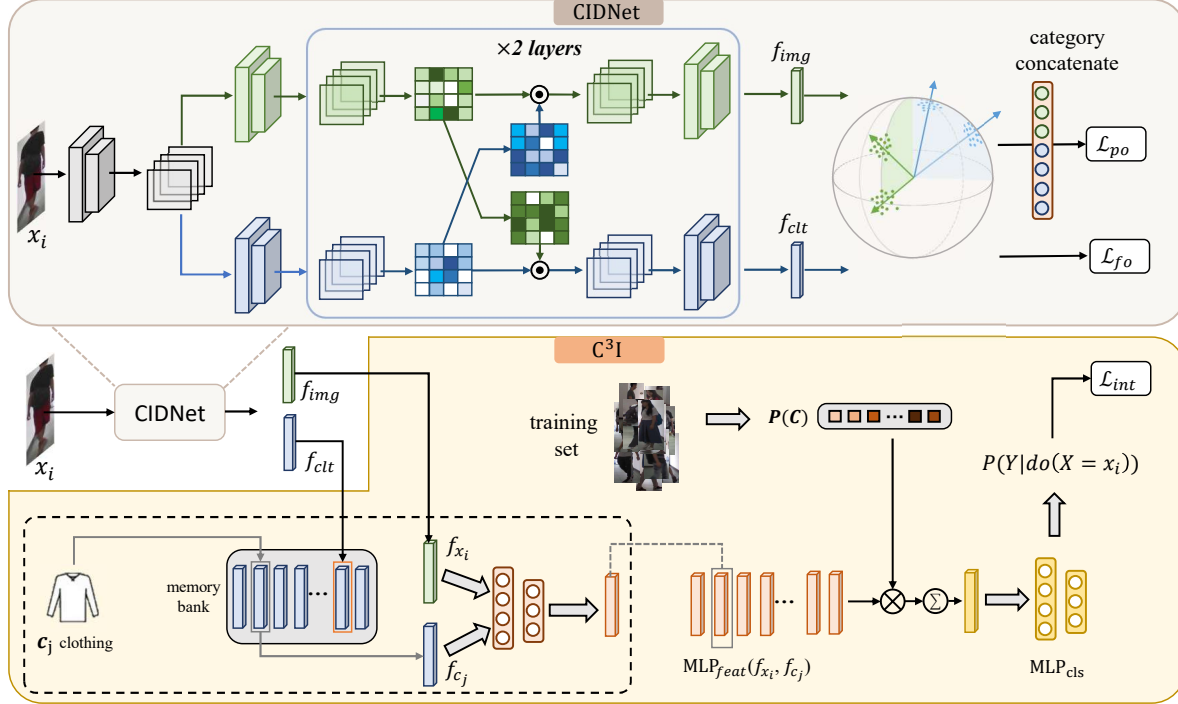


Figure 2. Framework overview of the proposed Causal Clothes-Invariant Learning (CCIL). The Clothes-Identity Disentangle Network (CIDNet) extracts discriminative and disentangled clothes features f_{clt} and image features f_{img} . The Causal Cloth-Changing Intervention (C^3I) module stores clothing descriptors for the entire dataset via memory bank and then eliminates the impact of identity-clothing spurious correlation through backdoor adjustments to achieve clothes-invariant feature learning.

away from the negative ones.

$$\mathcal{L}_{me} = \mathbb{E}[\max(\rho - \|f_m - f'_m\|_2, 0)] + \mathbb{E}[\|f_m - f'_m\|_2], m, \in \{img, clt\}, \quad (6)$$

where f_m represents the feature of m kind (clothes or images). f'_m is the feature center of the positive samples for f_m and f''_m is the negative one. and ρ is the margin parameter. Specifically, this loss is intended to keep features of the same identity or the same clothes close to each other and features of different identities or different clothes away from each other, thus making features more discriminative.

3.2.2 Causal intervention feature learning

For a CC-ReID training set \mathcal{T}_{train} , including N unique identities and M unique pieces of clothes, we propose to achieve the clothes-invariant feature learning by directly modeling the causal intervention probability $P(Y|do(X))$ rather than the likelihood one $P(Y|X)$, where X and Y denote the input images and corresponding human IDs, respectively. So the optimization pipeline of our method can be represented as minimizing the following loss function:

$$\mathcal{L}_{int} = \mathbb{E}_i [-\log P(Y = y_i | do(X = x_i))], \quad (7)$$

where y_i means the ground-truth identity of the image x_i .

Based on all these modules, in the training process, our loss function can be organized as follows:

$$\mathcal{L} = \mathcal{L}_{int} + \mathcal{L}_{int.kl} + \mathcal{L}_{cls} + \mathcal{L}_{kl} + \mathcal{L}_{me} \quad (8)$$

Note that we add an additional KL-divergence loss $\mathcal{L}_{int.kl}$ on the intervention probability to enhance predicted ID distributions, which is similar like we do before in the previous subsection. So the current key now is how to achieve the $P(Y|do(X = x_i))$. To treat that, we propose the Causal Cloth-Changing Intervention (C^3I).

3.3. Causal Cloth-Changing Intervention

3.3.1 Theoretical analysis

As can be seen from the Equation 1, to model the $P(Y|do(X))$, we need to model the $P(Y|X, C)$ and $P(C)$. $P(C)$ denotes the probabilities of each piece of clothing, which can be approximated on the training set. $P(Y|X, C)$ is more complex, so we model it by a neural network:

$$P(Y|X = x_i, C = c_j) = \text{MLP}(f_{x_i}, f_{c_j}). \quad (9)$$

where $\text{MLP}(\cdot, \cdot)$ means a Multiple Layer Perceptron (MLP) that takes the image features f_{x_i} and clothes features f_{c_j} to compute the probability distribution of ID. This kind of neural network can be interpreted as follows: Its last layer is the classifier and the other layers are the feature extractor.

So the equation of $P(Y|do(X))$ can be rewritten as:

$$\begin{aligned} P(Y|do(X = x_i)) &= \sum_{j=1}^M \text{MLP}(f_{x_i}, f_{c_j}) \cdot P(C = c_j) \\ &= \sum_{j=1}^M \text{MLP}_{cls}[\text{MLP}_{feat}(f_{x_i}, f_{c_j})] \cdot P(C = c_j). \end{aligned} \quad (10)$$

where $\text{MLP}_{cls}(\cdot)$ is the classifier consisting of a fully-connected layer with the softmax activation function and $\text{MLP}_{feat}(\cdot, \cdot)$ means a feature fusion module that combining the two features together, which can be easily implemented by concatenating two features first and then feeding the concatenated features into a fully-connected layer. To reduce the computational complexity, we follow [33, 37, 39] to utilize the Normalized Weighted Geometric Mean (NWGM) [35]:

$$P(Y|do(X = x_i)) \approx \text{MLP}_{cls} \left(\sum_{j=1}^M \text{MLP}_{feat}(f_{x_i}, f_{c_j}) \cdot P(C = c_j) \right), \quad (11)$$

This equation shows that we utilize a deep learning implementation (the right-hand term) to model the intervention probability (the left-hand term). If the right-hand term is really optimized to the ideal intervention probability, the feature f_{x_i} will become clothes-invariant.

To achieve the expectation that modeling the intervention probability by a deep learning implementation, the key is to ensure the establishment of Equation 9 as much as possible. So we investigate some basic conditions image feature f_{x_i} and clothes feature f_{c_j} should have. We go back to review their original function. From the Equation 9, we conclude that f_{x_i} and f_{c_j} should be cooperated with each other to help the MLP to model $P(Y|X = x_i, C = c_j)$ from the data. $P(Y|X = x_i, C = c_j)$ means the probability of the human identity conditioned on the i -th image x_i with the j -th clothing c_j . Mention that when we traverse the clothes in Equation 1, c_j can be any clothing, so it may not be the clothing worn by the person in x_i . From that analysis, we give the properties that f_{x_i} and f_{c_j} should have:

- (i) f_{x_i} must contain the human identity cues of x_i .
- (ii) f_{c_j} must contain rich and discriminative clothes information that can distinguish the c_j clothes from others.
- (iii) $\forall x_i \in \{x_1, x_2, \dots, x_N\}, c_j \in \{c_1, c_2, \dots, c_M\}$, it is better for f_{c_j} orthogonal to f_{x_i} mathematically.

The first property is based on the requirement of predicting ID distribution in $P(Y|X = x_i, C = c_j)$. If f_{x_i} does not contain the identity cues, the probability of Y cannot be inferred from x_i and c_j . The second property is matched that, in Equation 1, $P(Y|X = x_i, C = c_j)$ needs to be computed under different clothes ($j \in \{1, 2, \dots, M\}$). If f_{c_j} is not discriminative, $P(Y|X = x_i, C = c_j)$ will become trivial for different clothes and be close to $P(Y|X = x_i)$, even making our causal-based method is degenerated into the likelihood-based one. The third property is owing that

$P(Y|X = x_i, C = c_j)$ should be computed under combinations of different x_i and c_j . This means that different image features should cooperate with different clothes features. So it is better that the spanned space of image features F_X is orthogonal to the clothes one F_C . Because under such orthogonality, on the one hand, for different i , the changes of f_{x_i} will not affect f_{c_j} , and on the other hand, that F_C and F_X can represent all combinations of x_i and c_j completely.

3.3.2 Deep learning implementation

From the aforementioned analysis, we conclude three properties of the clothes and image features, that are critical to achieving the intervention. Fortunately, the disentangled features provided by the CIDNet satisfy those properties. The feature learning process of CIDNet ensures the discriminativeness of each kind of feature so that the clothes features contain clothes type information and the image features carry rich human identity information, which coincides with the properties (i) and (ii). And for the properties (iii) that two kinds of features preferably orthogonal, the disentangled features can also be satisfied to a certain extent because their semantic information is quite different.

So, for a specific image x_i , the CIDNet feedback the features f_{img} and f_{cld} . We let the f_{img} is equal to the f_{x_i} . For f_{cld} , it represents the clothes worn by the person in the image x_i . However, in Equation 11, we need to traverse all clothes, meaning that we need all clothes features to compute the intervention. It is time-consuming to extract all clothes features from the whole dataset in each iteration, so we build a memory bank [40] to store the clothes features and update them by exponential moving average (EMA):

$$f'_{c_k} = \alpha \cdot f_{c_k} + (1 - \alpha) \cdot f_{cld}, \quad (12)$$

where c_k is the clothes of the f_{cld} and α is the memory coefficient. We empirically set α to a value close to 1, *e.g.* 0.9, to achieve the balance of updating speed and stability. This memory bank is updated in each iteration and can provide us with all clothes features more effectively.

In conclusion, as shown in Figure 2, for a given image, CIDNet extracts the image and clothes features first. Then, the clothes features are used to update the corresponding clothes features in the memory bank. After that, the image features and clothes memory bank features are used to compute the Equation 11 and get the intervention probabilities $P(Y|do(X))$, which is used to compute \mathcal{L}_{int} and $\mathcal{L}_{int.kl}$

4. Experiments

4.1. Datasets and Evaluation Protocol

Datasets. In this section, we evaluate the proposed approach on three widely used CC-ReID datasets, *i.e.*, PRCC [36], LTCC [24] and VC-Clothes [32]. These public datasets are either synthetic or collected with the permission of the person being filmed and there is no ethical risk. PRCC contains 33,698 images of 221 identities with 442 pieces of clothing captured by 3 cameras. LTCC contains

Table 1. Comparison of rank-k accuracy (%) and mAP accuracy(%) with the state-of-the-art methods under the cloth-changing test setting. Different from other methods, original CAL performs a multi-shot testing protocol on PRCC. CAL[†] means that we use the author’s open source code for standard single-shot testing on PRCC or standard resolution training on all datasets to ensure a fair comparison.

Method	Modality	Resolution	PRCC		LTCC		VC-Clothes	
			Rank-1	Rank-10	Rank-1	mAP	Rank-1	mAP
LOMO+XQDA [18]	RGB	256×128	14.5	43.6	10.8	5.6	34.5	30.9
LOMO+KISSME [16]	RGB	256×128	18.6	49.8	11.0	5.3	35.7	31.3
ResNet-50 [8]	RGB	256×128	19.4	52.4	20.1	9.0	36.4	32.4
PCB [28]	RGB	384×192	22.9	61.2	23.5	10.0	62.0	62.2
CESD [24]	RGB+pose	384×192	-	-	25.2	12.4	-	-
SPT+ASE [36]	contour sketch	224×224	34.4	77.3	-	-	-	-
GI-ReID [13]	RGB+2D	256×128	37.6	82.3	23.7	10.4	64.5	57.8
3DSL [3]	RGB+pose+2D+3D	256×128	51.3	86.5	31.2	14.8	79.9	81.2
FSAM [9]	RGB+pose+2D	256×128	54.5	86.4	38.5	16.2	78.6	78.9
CAL [†] [7]	RGB	256×128	46.0	76.1	33.7	16.6	73.7	74.1
CAL [†] [7]	RGB	384×192	51.8	82.1	40.1	18.0	81.4	81.7
CCIL (ours)	RGB	256×128	58.2	86.7	39.2	18.1	80.4	79.6
CCIL (ours)	RGB	384×192	62.5	88.7	43.4	20.5	83.9	82.8

17,119 images of 152 identities with 477 pieces of clothing captured by 12 cameras. **VC-Clothes** is a synthetic CC-ReID dataset rendered by GTA5 game engine, which contains 19,060 images of 512 identities with 1,241 pieces of clothing captured by 4 cameras.

Evaluation Protocol. All the experiments follow the evaluation protocol in existing CC-ReID benchmarks. The cumulative matching characteristics (CMC) and mean average precision (mAP) are adopted as the evaluation metrics. For each dataset, we utilized the **cloth-changing test setting**, which means there are all cloth-changing samples in the testing set. For PRCC, we followed the single-shot evaluation protocol by randomly selecting one image per identity as a gallery and report the average performance for 10 repeated evaluations. As for the other two datasets, we followed the multi-shot evaluation protocol by choosing all the images of each identity as the gallery. And we also evaluated the performance in the **standard test setting**. For PRCC and VC-Clothes datasets, we used all cloth-consistent samples in the test set. While for the LTCC dataset, all samples including cloth-consistent and cloth-changing samples were used for testing.

4.2. Implementation Details

For the model, we adopt the ResNet-50 [8] pre-trained on ImageNet [4] as our backbone in the CIDNet. The branch-shared module is set as the 1st bottleneck of ResNet. And the 2nd, 3rd, and 4th bottlenecks are organized as branch-specific modules. Our S^2M is added after the 2nd and 3rd bottlenecks. Following the widely used Re-ID methods [20], the stride size of the last convolutional layer is set to 1, and a BNNeck is added before the classifier.

For optimization, random cropping, random horizontal flipping, and random erasing [42] are adopted for data augmentation. The optimizer is set as the Adam [15] with the warmup strategy that linearly increased the learning rate from $3.5e-5$ to $3.5e-4$ in the first 10 epochs. We then

decreased the learning rate by a factor of 10 at the 30th epoch. For PRCC we trained the model for 50 epochs, and for LTCC and VC-Clothes we trained the model for 100 epochs. Each batch contained 64 images of 8 identities. The margin hyper-parameter ρ in Equation. 6 is set to 0.6.

4.3. Comparison with State-of-the-art Methods

We compare our method with state-of-the-art (SOTA) cloth-changing ReID methods, including CESD [24], SPT+ASE [36], GI-ReID [13], 3DSL [3], FSAM [9] and CAL [7]. As shown in Table 1, our method achieves excellent performance in all three CC-ReID datasets under the cloth-changing test setting.

Compared with the methods using auxiliary modality data, our method surpasses the SOTA method FSAM by 3.7% / 0.7% / 1.8% in Rank-1 accuracy on PRCC/LTCC/VC-Clothes datasets. Our method does not introduce other modality data or modules to extract such modalities for constraining features, but we still achieve better results. The main reason is that although these methods introduced auxiliary clothes-invariant modality information, *e.g.*, poses and contours, into the features, they cannot avoid the fact that the likelihood-based methods carry the clothes-variant shortcut unavoidably. So they cannot provide further satisfying results while our causality-based methods could. It proves the effectiveness of our methods and also shows the priority of the causality-based models.

Compared with the methods using RGB modality only, our method outperformed CAL by a large margin on the standard-resolution (256×128) images, with 12.2% / 5.5% / 6.7% absolute improvement in rank-1 accuracy on PRCC/LTCC/VC-Clothes datasets. Additional comparisons on high-resolution (384×192) images also demonstrate the absolute advantage of our approach, which also surpasses CAL by 10.7% / 3.3% / 2.5% in rank-1 accuracy on PRCC/LTCC/VC-Clothes datasets. From our aforementioned analysis in § 1, it is challenging for the likelihood-

Table 2. The results on standard test setting.

Method	PRCC		LTCC		VC-Clothes	
	Rank-1	mAP	Rank-1	mAP	Rank-1	mAP
PCB [28]	86.9	98.8	65.1	30.6	94.7	94.3
FSAM [9]	98.8	100	73.2	35.4	94.7	94.8
CAL [†] [7]	99.0	100	72.4	38.7	94.5	95.1
Baseline	97.2	100	61.5	27.9	94.2	94.4
CCIL(ours)	98.8	100	72.5	36.9	95.4	95.2

Table 3. Ablation study on PRCC dataset. The important modules of the proposed CCIL, *i.e.*, CIDNet, and C³I are analyzed under different settings.

i	S^2M	JPS	L_{kl}	L_{me}	C ³ I	Rank-1	Rank-10
1	-	-	-	-	-	45.9	77.1
2	✓	-	-	-	-	48.8	79.7
3	✓	✓	-	-	-	50.0	81.1
4	✓	✓	✓	-	-	54.8	83.1
5	✓	✓	✓	✓	-	56.1	83.7
6	-	-	-	-	✓	47.2	78.6
7	✓	-	-	-	✓	50.5	81.0
8	✓	✓	-	-	✓	53.2	83.1
9	✓	✓	✓	-	✓	56.5	84.6
10	✓	✓	✓	✓	✓	58.2	86.7

Table 4. Ablation study on PRCC dataset for C³I and its variants.

i	Method	Rank-1	Rank-10
0	No causal	56.1	83.7
1	C ³ I→MLP	55.5	83.3
2	Memory→Random	56.3	84.1
3	Memory→Learnable weight	55.4	83.0
4	Ours (C ³ I)	58.2	86.7

based methods to drop clothes-related cues while keeping the identity discriminativeness. CAL also has focused on and reported the conflict between the clothes-invariant and the identity discriminativeness [7] and it tried to solve it by adding well-designed constraints in the traditional likelihood framework. But from our results, it can be seen that it is still challenging for the likelihood-based methods to achieve better clothes-invariant representations, further proving the effectiveness of our causality-based work.

The experiment results on the standard test setting are presented in Table 2. Our method obtains a consistent improvement compared to the baseline model, improving Rank1 accuracy by 1.6%/10.0%/1.2% on PRCC/LTCC/VC-Clothes datasets, respectively. Compared to other ReID methods, our method has better or at least comparable performance on standard test setting, which also demonstrates the excellent generalizability of our method.

4.4. Ablation Study

In this section, we conduct an ablation study on the large-scale dataset PRCC to prove the effectiveness of the modules of the proposed CCIL—CIDNet and C³I.

Effectiveness of CIDNet. In our proposed CCIL, we introduce a CIDNet to obtain two discriminative and disentangled representations f_{img} and f_{cIt} from the same image. As

shown in Table 3, we evaluate the effectiveness of each detailed part of CIDNet. Although the CIDNet is designed for the causal intervention requirement, it can be understood as a specific kind of disentangle system that still can provide effective image features. In this subsection, we do the ablation studies for the CIDNet under two different scenarios, with C³I and without C³I, to show its effectiveness. The 1st line is our baseline, a two-stream network without any other modules and trained by the standard cross-entropy loss.

Experiments in 1st~5th lines are done without the causal module C³I. It demonstrates the effectiveness of our CIDNet as a traditional likelihood-based network. Compared with the 2nd line, it can be seen that S^2M can bring about 2.9% / 2.6% gains on rank-1 / rank-10 accuracy. It is because S^2M constrains image features do not focus on the region attended by the clothes features, equal to guiding the image features to become clothes-invariant to a certain degree. And from the 3rd, 4th and 5th lines, JPS, L_{kl} and L_{me} bring additional 1.2%, 4.8% and 1.3% improvements in rank-1 accuracy, respectively. It proves that JPS effectively helps to disentangle features, while L_{kl} and L_{me} further increase the discriminativeness of the image feature, leading to more robust retrieval results and proving their positive functions to our backbone feature extractor.

Experiments in 6th~10th lines are with the C³I. These experiments aim to show promotes provided by the CIDNet to our causal intervention module. From the 1st line and the 6th line, we can find that our causal intervention module C³I delivers a 1.3% / 1.5% improvement on rank-1 / rank-10 accuracy for our baseline system. And comparing those improvements with the gains derived from the 5th and 10th lines, it can be seen that with the discriminativeness and orthogonality properties introduced by the CIDNet, although the backbone network becomes stronger, our C³I further brings greater gains, about 2.1% and 3.0% improvement on rank-1 and rank-10 metric, respectively. This, on the one hand, proves that our concluded properties actually match the requirement of the causal intervention implementation, on the other hand, it demonstrates that CIDNet does indeed achieve such properties effectively.

Effectiveness of C³I. Comparing the 1st~5th and 6th~10th in Table 3 one by one, it can be seen that our C³I can also improve the performance under different backbone networks. To further prove that the reason for the performance gain provided by C³I is causality rather than introducing other parameters, we conduct a series of further experiments in Table 4. The 1st line corresponds that we replace C³I with the common MLP. This experiment aims to show what happens when we delete the causal intervention training scheme but keep the total parameter not changed. The results show that it brings a performance drop of 2.7% / 3.4% on rank-1 / rank-10 accuracy compared with our C³I. Except that, when compared with only using our backbone, 0th line in Table 4, this MLP even introduces little performance drop because, without the causal intervention training scheme, this MLP is equal to explicitly introducing the clothes information, further increasing the clothes

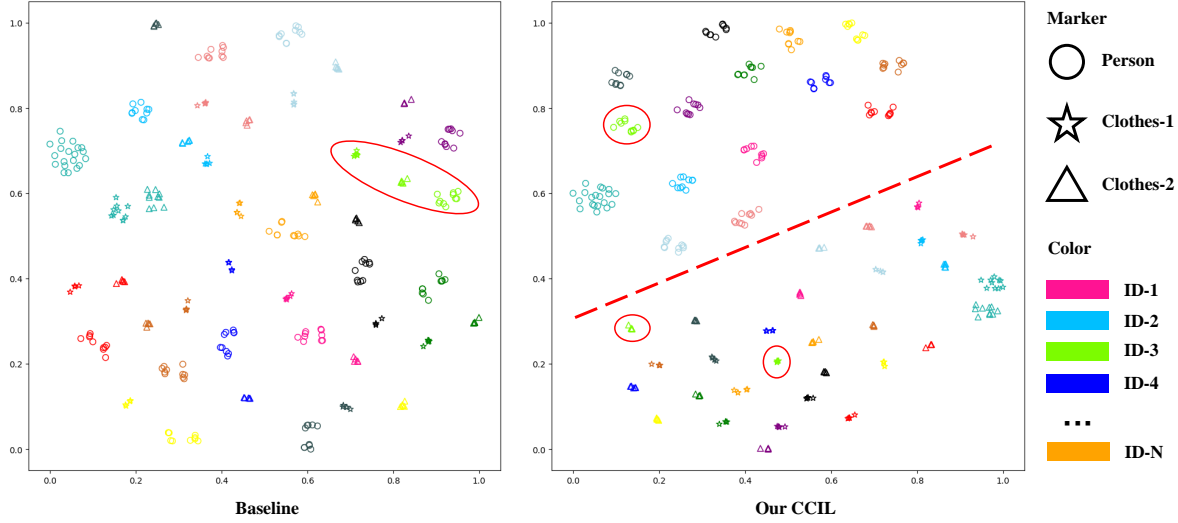


Figure 3. t-SNE [31] visualization of the distributions of image features f_{img} and clothes features f_{clt} on PRCC dataset. Different colors represent different identities. Circle, triangle, and star represent a person and his/her first and second sets of clothes, respectively.

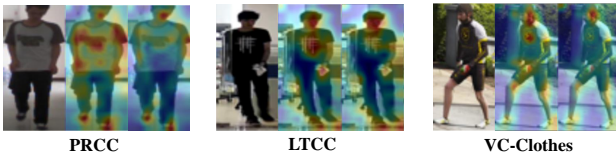


Figure 4. Visualization of the activation feature maps. In each triplet, the 2nd and 3rd columns present the activation maps of the baseline and our CCIL, respectively.

information carries by the likelihood-based methods. But when changing the training target from the likelihood to the causal intervention, although this MLP is quite shallow, the whole framework of the model has been changed a lot. So the results have significant improvements, further proving the effectiveness of our causality-based model.

In addition, we investigate the effectiveness of achieving the memory bank. The experiment results in the 2nd line, we use a randomly initialized vector as the value in the memory bank and keep it fixed. This process only introduces some performance jitters, which is trivial compared with no causality (0th line). And in the 3rd line, we instead treat the memory bank as a learnable parameter. This treatment even introduces performance dropping compared with no causality (0th line). This is because the memory bank parameters learned by backpropagation do not have effective constraints to preserve our concluded properties for the clothes features, such as discriminative and orthogonal to image features, making the optimization target have a certain deviation from the ideal causal intervention. All these ablation experiments demonstrate the effectiveness of our C³I design for achieving the causal intervention.

5. Visualization

Visualization of feature distribution. Figure 3 shows t-SNE [31] visualization results for f_{img} and f_{clt} . In the feature distribution of the baseline model, person features (circles) and clothing features (triangles and stars) are mixed together. It shows that the baseline extracted f_{img} and f_{clt} have a strong correlation. On the contrary, our method perfectly distinguishes person features and clothing features, and it is easy to find a line to separate them in the figure. In addition, different clothes belonging to the same person are also better distinguished. This proves that the method makes f_{img} and f_{clt} orthogonal and f_{clt} well distinguished from each other, which satisfies our concluded 3 properties of such features for the causal intervention.

Visualization of the activation feature maps. As shown in Figure 4, we visualize three groups of activation feature maps on different datasets. Our approach focuses on the distinct details of each identity such as the head, hands, feet, and joints while neglecting the clothes-related regions compared to the baseline.

6. Conclusion

In this paper, we propose a Causal Clothes-Invariant Learning (CCIL) to tackle Clothes-Changing Person Re-identification. The proposed method includes a well-designed Clothes-Identity Disentangle Network (CIDNet) and a novel Causal Cloth-Changing Intervention (C³I) module. The CIDNet extracts discriminative and disentangled clothing and image features. Then, the C³I utilizes those features to train the model under the causal intervention framework rather than traditional likelihood-based manners, achieving better clothes-invariant features. These two main contributions are complementary to each other and achieve a new state of the art.

References

- [1] Elias Bareinboim and Judea Pearl. Controlling selection bias in causal inference. In *Artificial Intelligence and Statistics*, pages 100–108. PMLR, 2012. 2
- [2] Krzysztof Chalupka, Pietro Perona, and Frederick Eberhardt. Visual causal feature learning. *arXiv preprint arXiv:1412.2309*, 2014. 2
- [3] Jiaxing Chen, Xinyang Jiang, Fudong Wang, Jun Zhang, Feng Zheng, Xing Sun, and Wei-Shi Zheng. Learning 3d shape feature for texture-insensitive person re-identification. In *Proceedings of the IEEE/CVF Conference on Computer Vision and Pattern Recognition*, pages 8146–8155, 2021. 2, 6
- [4] Jia Deng, Wei Dong, Richard Socher, Li-Jia Li, Kai Li, and Li Fei-Fei. Imagenet: A large-scale hierarchical image database. In *2009 IEEE conference on computer vision and pattern recognition*, pages 248–255, 2009. 6
- [5] Madelyn Glymour, Judea Pearl, and Nicholas P Jewell. *Causal inference in statistics: A primer*. John Wiley & Sons, 2016. 1, 2
- [6] Shaogang Gong, Marco Cristani, Chen Change Loy, and Timothy M Hospedales. The re-identification challenge. In *Person re-identification*, pages 1–20. 2014. 1, 2
- [7] Xinqian Gu, Hong Chang, Bingpeng Ma, Shutao Bai, Shiguang Shan, and Xilin Chen. Clothes-changing person re-identification with rgb modality only. In *Proceedings of the IEEE/CVF Conference on Computer Vision and Pattern Recognition*, pages 1060–1069, 2022. 2, 6, 7
- [8] Kaiming He, Xiangyu Zhang, Shaoqing Ren, and Jian Sun. Deep residual learning for image recognition. In *Proceedings of the IEEE conference on computer vision and pattern recognition*, pages 770–778, 2016. 6
- [9] Peixian Hong, Tao Wu, Ancong Wu, Xintong Han, and Wei-Shi Zheng. Fine-grained shape-appearance mutual learning for cloth-changing person re-identification. In *Proceedings of the IEEE/CVF Conference on Computer Vision and Pattern Recognition*, pages 10513–10522, 2021. 2, 6, 7
- [10] Houjing Huang, Dangwei Li, Zhang Zhang, Xiaotang Chen, and Kaiqi Huang. Adversarially occluded samples for person re-identification. In *Proceedings of the IEEE Conference on Computer Vision and Pattern Recognition*, pages 5098–5107, 2018. 2
- [11] Yan Huang, Qiang Wu, JingSong Xu, Yi Zhong, and ZhaoXiang Zhang. Clothing status awareness for long-term person re-identification. In *Proceedings of the IEEE/CVF International Conference on Computer Vision*, pages 11895–11904, 2021. 2
- [12] Yukun Huang, Zheng-Jun Zha, Xueyang Fu, and Wei Zhang. Illumination-invariant person re-identification. In *Proceedings of the 27th ACM international conference on multimedia*, pages 365–373, 2019. 2
- [13] Xin Jin, Tianyu He, Kecheng Zheng, Zhiheng Yin, Xu Shen, Zhen Huang, Ruoyu Feng, Jianqiang Huang, Xian-Sheng Hua, and Zhibo Chen. Cloth-changing person re-identification from a single image with gait prediction and regularization. *arXiv preprint arXiv:2103.15537*, 2021. 2, 6
- [14] Srikrishna Karanam, Yang Li, and Richard J Radke. Person re-identification with discriminatively trained viewpoint invariant dictionaries. In *Proceedings of the IEEE international conference on computer vision*, pages 4516–4524, 2015. 2
- [15] Diederik P Kingma and Jimmy Ba. Adam: A method for stochastic optimization. *arXiv preprint arXiv:1412.6980*, 2014. 6
- [16] Martin Koestinger, Martin Hirzer, Paul Wohlhart, Peter M Roth, and Horst Bischof. Large scale metric learning from equivalence constraints. In *2012 IEEE conference on computer vision and pattern recognition*, pages 2288–2295, 2012. 6
- [17] Xulin Li, Yan Lu, Bin Liu, Yating Liu, Guojun Yin, Qi Chu, Jinyang Huang, Feng Zhu, Rui Zhao, and Nenghai Yu. Counterfactual intervention feature transfer for visible-infrared person re-identification. 2
- [18] Shengcai Liao, Yang Hu, Xiangyu Zhu, and Stan Z Li. Person re-identification by local maximal occurrence representation and metric learning. In *Proceedings of the IEEE conference on computer vision and pattern recognition*, pages 2197–2206, 2015. 6
- [19] David Lopez-Paz, Robert Nishihara, Soumith Chintala, Bernhard Scholkopf, and Léon Bottou. Discovering causal signals in images. In *Proceedings of the IEEE Conference on Computer Vision and Pattern Recognition*, pages 6979–6987, 2017. 2
- [20] Hao Luo, Youzhi Gu, Xingyu Liao, Shenqi Lai, and Wei Jiang. Bag of tricks and a strong baseline for deep person re-identification. In *Proceedings of the IEEE/CVF Conference on Computer Vision and Pattern Recognition Workshops*, pages 0–0, 2019. 1, 2, 6
- [21] Yulei Niu, Kaihua Tang, Hanwang Zhang, Zhiwu Lu, Xian-Sheng Hua, and Ji-Rong Wen. Counterfactual vqa: A cause-effect look at language bias. In *Proceedings of the IEEE/CVF Conference on Computer Vision and Pattern Recognition*, pages 12700–12710, 2021. 2
- [22] Judea Pearl and Dana Mackenzie. *The book of why: the new science of cause and effect*. Basic books, 2018. 1, 2
- [23] Jiaxin Qi, Yulei Niu, Jianqiang Huang, and Hanwang Zhang. Two causal principles for improving visual dialog. In *Proceedings of the IEEE/CVF Conference on Computer Vision and Pattern Recognition*, pages 10860–10869, 2020. 2
- [24] Xuelin Qian, Wenxuan Wang, Li Zhang, Fangrui Zhu, Yanwei Fu, Tao Xiang, Yu-Gang Jiang, and Xiangyang Xue. Long-term cloth-changing person re-identification. In *Proceedings of the Asian Conference on Computer Vision*, 2020. 2, 5, 6
- [25] Yongming Rao, Guangyi Chen, Jiwen Lu, and Jie Zhou. Counterfactual attention learning for fine-grained visual categorization and re-identification. In *Proceedings of the IEEE/CVF International Conference on Computer Vision*, pages 1025–1034, 2021. 2
- [26] M Saquib Sarfraz, Arne Schumann, Andreas Eberle, and Rainer Stiefelwagen. A pose-sensitive embedding for person re-identification with expanded cross neighborhood re-ranking. In *Proceedings of the IEEE conference on computer vision and pattern recognition*, pages 420–429, 2018. 2
- [27] Yifan Sun, Changmao Cheng, Yuhan Zhang, Chi Zhang, Liang Zheng, Zhongdao Wang, and Yichen Wei. Circle loss: A unified perspective of pair similarity optimization. In *Proceedings of the IEEE/CVF Conference on Computer Vision and Pattern Recognition*, pages 6398–6407, 2020. 2
- [28] Yifan Sun, Liang Zheng, Yi Yang, Qi Tian, and Shengjin Wang. Beyond part models: Person retrieval with refined part pooling (and a strong convolutional baseline). In *Pro-*

ceedings of the European conference on computer vision (ECCV), pages 480–496, 2018. 1, 2, 6, 7

of the AAAI Conference on Artificial Intelligence, volume 34, pages 13001–13008, 2020. 6

- [29] Kaihua Tang, Jianqiang Huang, and Hanwang Zhang. Long-tailed classification by keeping the good and removing the bad momentum causal effect. *arXiv preprint arXiv:2009.12991*, 2020. 2
- [30] Kaihua Tang, Yulei Niu, Jianqiang Huang, Jiaxin Shi, and Hanwang Zhang. Unbiased scene graph generation from biased training. In *Proceedings of the IEEE/CVF Conference on Computer Vision and Pattern Recognition*, pages 3716–3725, 2020. 2
- [31] Laurens Van der Maaten and Geoffrey Hinton. Visualizing data using t-sne. *Journal of machine learning research*, 9(11), 2008. 8
- [32] Fangbin Wan, Yang Wu, Xuelin Qian, Yixiong Chen, and Yanwei Fu. When person re-identification meets changing clothes. In *Proceedings of the IEEE/CVF Conference on Computer Vision and Pattern Recognition Workshops*, pages 830–831, 2020. 2, 5
- [33] Tan Wang, Jianqiang Huang, Hanwang Zhang, and Qianru Sun. Visual commonsense r-cnn. In *Proceedings of the IEEE/CVF Conference on Computer Vision and Pattern Recognition*, pages 10760–10770, 2020. 2, 5
- [34] Yan Wang, Lequn Wang, Yurong You, Xu Zou, Vincent Chen, Serena Li, Gao Huang, Bharath Hariharan, and Kilian Q Weinberger. Resource aware person re-identification across multiple resolutions. In *Proceedings of the IEEE conference on computer vision and pattern recognition*, pages 8042–8051, 2018. 2
- [35] Kelvin Xu, Jimmy Ba, Ryan Kiros, Kyunghyun Cho, Aaron Courville, Ruslan Salakhudinov, Rich Zemel, and Yoshua Bengio. Show, attend and tell: Neural image caption generation with visual attention. In *International conference on machine learning*, pages 2048–2057. PMLR, 2015. 5
- [36] Qize Yang, Ancong Wu, and Wei-Shi Zheng. Person re-identification by contour sketch under moderate clothing change. *IEEE transactions on pattern analysis and machine intelligence*, 43(6):2029–2046, 2019. 2, 5, 6
- [37] Xu Yang, Hanwang Zhang, Guojun Qi, and Jianfei Cai. Causal attention for vision-language tasks. In *Proceedings of the IEEE/CVF Conference on Computer Vision and Pattern Recognition*, pages 9847–9857, 2021. 5
- [38] Shijie Yu, Shihua Li, Dapeng Chen, Rui Zhao, Junjie Yan, and Yu Qiao. Cocas: A large-scale clothes changing person dataset for re-identification. In *Proceedings of the IEEE/CVF Conference on Computer Vision and Pattern Recognition*, pages 3400–3409, 2020. 2
- [39] Dong Zhang, Hanwang Zhang, Jinhui Tang, Xiansheng Hua, and Qianru Sun. Causal intervention for weakly-supervised semantic segmentation. *arXiv preprint arXiv:2009.12547*, 2020. 2, 5
- [40] Hua Zhang, Liqiang Xiao, Xiaochun Cao, and Hassan Foroosh. Multiple adverse weather conditions adaptation for object detection via causal intervention. *IEEE Transactions on Pattern Analysis and Machine Intelligence*, 2022. 2, 5
- [41] Xuan Zhang, Hao Luo, Xing Fan, Weilai Xiang, Yixiao Sun, Qiqi Xiao, Wei Jiang, Chi Zhang, and Jian Sun. Aligned: Surpassing human-level performance in person re-identification. *arXiv preprint arXiv:1711.08184*, 2017. 1, 2
- [42] Zhun Zhong, Liang Zheng, Guoliang Kang, Shaozi Li, and Yi Yang. Random erasing data augmentation. In *Proceedings*